Magnetic moments, coupling, and interface interdiffusion in Fe/V(001) superlattices

M. M. Schwickert
Department of Physics and Astronomy, Ohio University, Athens, Ohio 45701

R. Coehoorn
Philips Research Laboratories, Prof. Holstlaan 4, 5656 AA Eindhoven, The Netherlands

M. A. Tomaz
Department of Physics and Astronomy, Ohio University, Athens, Ohio 45701

E. Mayo and D. Lederman
Department of Physics, West Virginia University, Morgantown, West Virginia 26506-6315

W. L. O'Brien
Synchrotron Radiation Center, University of Wisconsin-Madison, 3731 Schneider Drive, Stoughton, Wisconsin 53589

Tao Lin and G. R. Harp
Department of Physics and Astronomy, Ohio University, Athens, Ohio 45701
(Received 28 October 1997)

Epitaxial Fe/V(001) multilayers are studied both experimentally and by theoretical calculations. Sputter-deposited epitaxial films are characterized by x-ray diffraction, magneto-optical Kerr effect, and x-ray magnetic circular dichroism. These results are compared with first-principles calculations modeling different amounts of interface interdiffusion. The exchange coupling across the V layers is observed to oscillate, with antiferromagnetic peaks near the V layer thicknesses $t_V \approx 22$, 32, and 42 Å. For all films including superlattices and alloys, the average V magnetic moment is antiparallel to that of Fe. The average V moment increases slightly with increasing interdiffusion at the Fe/V interface. Calculations modeling mixed interface layers and measurements indicate that all V atoms are aligned with one another for $t_V \lesssim 15$ Å, although the magnitude of the V moment decays toward the center of the layer. This ''transient ferromagnetic'' state arises from direct (d-d) exchange coupling between V atoms in the layer. It is argued that the transient ferromagnetism suppresses the first antiferromagnetic coupling peak between Fe layers, expected to occur at $t_V \approx 12$ Å. [S0163-1829(98)06021-4]

I. INTRODUCTION

Vanadium stands at the edge of magnetism in the $3d$ transition metals. The five elements to the right of V in the periodic table are either antiferromagnetic (Cr, Mn) or ferromagnetic (Fe, Co, Ni) near or above room temperature. It is well known from neutron-diffraction studies[1,2] and electronic structure calculations[3] that V atoms, when dissolved in Fe, acquire a sizable induced magnetic moment: $\approx -1\,\mu_B$ in the dilute limit (with respect to the Fe moments in the host metal). Similarly, V is known to acquire a significant magnetic moment in close proximity to Fe in thin films,[4,5] polycrystalline multilayers,[6] or superlattices.[7] Here we probe the induced V moment when it is layered with Fe. The thickness dependence of the V moment provides a measure of its tendency toward ferromagnetism.

Generally, magnetic superlattices possess properties distinct from alloys with the same average composition. This is easily understood since random alloys have an average translational symmetry in 3D while superlattices are modulated along the z axis. ''Perfect'' superlattices comprise 2D layers of pure material with abrupt interfaces. Most theoretical studies have focused on perfect superlattices which, while simplifying calculations, are experimentally unattainable.

In this article, we use both experimental and theoretical studies of (001) oriented Fe/V to characterize the V magnetization over the entire spectrum of interface interdiffusion—from the random alloy to the perfect superlattice. We show that interdiffusion enhances the V magnetic moments as compared with perfect superlattices. This highlights the importance of performing calculations on more realistic structures, as is done here.

The V magnetic moments are aligned antiparallel to those in the Fe and decay monotonically, extending $\gtrsim 6$ Å (4 ML) away from each Fe interface. We term this a ''transient ferromagnetic'' state.

Magnetometry reveals exchange coupling between Fe layers that oscillates as a function of V layer thickness. Three antiferromagnetic (AF) coupling peaks are observed at ≈ 22, 32, and 42 Å. Another AF coupling peak expected for 12 Å V thickness is suppressed, possibly by the transient ferromagnetic behavior of V in these multilayers.

II. THEORY

Previous theoretical studies of Fe/V(001) superlattices are not in agreement regarding the magnetic state of V. Whereas

TABLE I. Calculated magnetic moments from [Fe 5 ML/V n ML] superlattices with perfect interfaces. Magnetic moments are in units of μ_B per atom. The layers labeled ''*I*'' are interface layers, while other layers are labeled with their distance from the interface. Thus, Fe *I*–2 is the atomic layer in the center of the Fe layer. As discussed in more detail in the text, the results indicated with $n=11^*$ refer to a superlattice in which the Fe sublattice, and not the V sublattice, is tetragonally deformed.

n	Fe *I*–2	Fe *I*–1	Fe I	V I	V I–1	V I–2	V I–3	V I–4	V I–5	Fe Avg.	V Avg.
1	2.33	2.46	1.90	−1.05						2.21	−1.05
3	2.31	2.44	1.76	−0.53	−0.08					2.14	−0.38
5	2.29	2.43	1.79	−0.49	−0.02	0.05				2.15	−0.19
7	2.27	2.39	1.83	−0.45	−0.08	0.00	0.00			2.14	−0.15
9	2.28	2.42	1.77	−0.50	−0.05	0.02	0.00	−0.01		2.13	−0.12
11	2.28	2.43	1.80	−0.48	−0.05	0.02	0.01	0.00	−0.01	2.15	−0.09
11*	2.24	2.38	1.75	−0.52	−0.03	−0.01	−0.02	0.01	0.03	2.10	−0.10

an early study[8] indicated an induced, transient ferromagnetic V state, a later study[9] indicated layer antiferromagnetism in the V interlayer. Recent first-principles calculations[10] indicate again a transient ferromagnetic V state. From all studies it follows that the interfacial V atoms have their magnetic moments aligned antiparallel to the Fe. Here we follow up the latter calculations, with special attention given to the effects of Fe-V interdiffusion. It is shown from the calculations that diffusion suppresses the formation of a transient antiferromagnetic state in the V layer, leading to a transient ferromagnetic state like that observed in experiments.

The calculations were performed using the augmented spherical wave method. Calculational details concerning the treatment of exchange and correlation, atomic sphere radii, basis sets, and Brillouin-zone scanning are as described in Ref. 10. The calculations give predictions for the magnetic moments at zero temperature, and only ferromagnetic alignment between adjacent Fe layers was considered. Two sets of calculations were performed, the first on perfect Fe/V(001) superlattices of the type 5 ML Fe/*n* ML V, with $n=1$, 3, 5, 7, 9, and 11, and the second on Fe/V(001) superlattices with an ordered mixed monolayer at the interfaces with an Fe:V concentration ratio of 1:1, of the type 4 ML Fe/ 1 ML $Fe_{0.5}V_{0.5}/(n-1)$ ML V/1 ML $Fe_{0.5}V_{0.5}$, with $n=1$, 3, 5, 7, 9, and 11. The method for choosing the atomic positions of the Fe and V atoms, which have in the elemental metals atomic radii that differ by 5.6%, is in both cases identical to the method used in Ref. 10: the Fe sublattice is cubic (undeformed), with interatomic distances equal to those in elemental Fe, whereas the V sublattice is assumed to be tetragonally distorted, fitting coherently with the Fe sublattice and with the c/a ratio taken such that the volume per V atom is equal to that in bulk V. This implies that the distance between the V layers is 11% larger than in bulk V. In order to check the sensitivity of the moments calculated to the deformation of the V sublattice, a calculation was carried out for a [Fe 5 ML/V 11 ML] ideal superlattice for which the V sublattice was cubic, with lattice parameters equal to those of elemental V, and the Fe sublattice was deformed, with the c/a ratio such that the volume per Fe atom is equal to that in bulk Fe.

For the second set of calculations (mixed interfaces) the unit cell was orthorhombic, with a lateral unit cell having dimensions $a_{Fe}\times 2a_{Fe}$. Within the mixed interface layer alternate rows of sites parallel to the [100] direction are occupied by Fe and V atoms. This corresponds to the structure as shown in Ref. 10 (Fig. 2, case $x=\frac{1}{2}$, structure II). This leads to two crystallographically distinct sites within each atomic layer, one [that we call (a)] at a lateral position at which the Fe layer is locally 6 ML thick, and one [that we call (b)] at a lateral position at which the Fe layer is locally 4 ML thick. The numerical accuracy of the Fe and V moments is $\pm 0.02\mu_B$ and $\pm 0.01\mu_B$, respectively.

The results of these calculations are presented in Tables I and II. Although there is a redistribution of the Fe magnetic moments, note that the average Fe moment is hardly changed from the bulk level. In all cases, the calculations show a net negative V moment, indicating that it is aligned antiparallel to the Fe. The V moment is largest close to the interfaces, and decreases away from the Fe interface with a decay that is quicker for perfect superlattices. Moreover, the layers with perfect interfaces show a slight tendency towards an oscillatory spin density that is not present in the calculations with diffused interfaces. This is evidence for the suppression of transient antiferromagnetism caused by frustration, as mentioned above.

We note that the results for the system [Fe 5 ML/V 11 ML] with a cubic V sublattice and a deformed Fe sublattice (indicated in Table I with the label 11*) are only marginally different from those for systems in which the V sublattice is deformed and the Fe sublattice is cubic.

III. SAMPLE PREPARATION

The superlattices were deposited by magnetron sputter deposition in an ultrahigh vacuum system (base pressure $<5\times 10^{-10}$ Torr) at Ohio University. Sputtering was performed in an Ar ambient of 3×10^{-3} Torr, with deposition rates near 0.5 Å/s. All samples were deposited on MgO(001) substrates, which were briefly repolished using 0.05μ alumina paste and rinsed before insertion into the vacuum system. The substrates were outgassed for ≈ 20 min at 870 K prior to deposition, and then coated with a 25 Å buffer layer of either Fe or Cr at that temperature. All samples were prepared with 20 Fe/V bilayers except where noted.

The samples were then allowed to cool in vacuum. The highest quality Fe/V interfaces were achieved by then depositing a 300 Å Cr-V alloy at 570 K. This alloy has a lattice constant inbetween those of Fe and V. An [Fe 10 Å/ V t_V] superlattice was subsequently deposited at 570 K. In agreement with Ref. 11, we find that this was the optimal growth temperature.

The above described samples were compared with similar

TABLE II. Calculated magnetic moments from [Fe 4 ML/FeV 1 ML/V n-1 ML/FeV 1 ML] superlattices, simulating diffused interfaces. Because there are two inequivalent sites in each monolayer depending on nearest or next-nearest-neighbor occupation, there are two magnetic moment values quoted for each layer (a, b). See the text for further details.

n	Fe I–1	Fe I	Fe mixed	V mixed	V I	V I–1	V I–2	V I–3	V I–4	Fe Avg.	V Avg.
1 *a*	2.44	2.11	2.05							2.19	−0.88
1 *b*	2.36	1.99		−0.88							
3 *a*	2.38	2.11	2.05		−0.28					2.09	−0.43
3 *b*	2.36	1.99		−0.72	−0.28						
5 *a*	2.38	2.03	1.52		−0.25	−0.05				2.07	−0.27
5 *b*	2.36	2.03		−0.76	−0.23	−0.04					
7 *a*	2.38	2.03	1.50		−0.26	−0.08	−0.01			2.06	−0.20
7 *b*	2.36	2.03		−0.78	−0.24	−0.04	−0.02				
9 *a*	2.39	2.05	1.55		−0.24	−0.07	−0.01	−0.02		2.08	−0.16
9 *b*	2.36	2.05		−0.78	−0.24	−0.04	−0.01	−0.02			
11 *a*	2.39	2.05	1.54		−0.24	−0.07	−0.00	−0.01	−0.01	2.08	−0.13
11 *b*	2.36	2.05		−0.78	−0.23	−0.04	−0.01	−0.01	−0.01		

[Fe 7.5 Å/V t_V] superlattices deposited directly onto the 25 Å high-temperature buffer layer, and with a growth temperature of 370 K. The 370 K samples showed greater interface roughness or interdiffusion, as determined by x-ray diffraction (see below). Finally, (001) oriented random Fe-V alloys were prepared by codeposition onto the high-temperature buffer layer at 570 K. Some superlattices (and alloys) were deposited as ''wedged'' samples, where the V layer thickness (alloy composition) varied with position along the substrate. This permits direct comparison between superlattices (alloys) grown under identical growth conditions. Other samples were prepared with uniform V layer thicknesses to permit detailed x-ray studies.

All samples were coated with a final layer of either 20 Å Al, or 20 Å Si_3N_4 to prevent oxidation after removal from vacuum. The layer thicknesses were controlled with *in situ* crystal thickness monitors near each sputter source. These monitors had been previously calibrated with the growth of a thick film, whose thickness was independently measured by step profilometry. Additionally, electron stimulated x-ray fluorescence was used to verify thicknesses after growth. X-ray-diffraction superlattice features also provided complimentary information regarding layer thicknesses. The results from all these techniques were combined to give the best estimates of layer thicknesses and compositions.

IV. X-RAY DIFFRACTION

The structural quality of the superlattices was characterized by x-ray diffraction on samples prepared with uniform layer thicknesses. Figure 1 presents high-angle diffraction data taken from two samples prepared especially for x-ray diffraction having 40 bilayer periods. These scans were taken with a fixed-anode diffractometer with 1° angular resolution and Cu K_α radiation. The 570 K sample incorporated a [9 Å V/43 Å Fe]$_{40}$ superlattice, while the 370 K sample has a [27 Å V/7.5 Å Fe]$_{40}$ superlattice. Both spectra show only diffraction peaks associated with the (001) superlattice, and the MgO substrate, witnessing a single growth orientation.

Low-angle diffraction scans from the same two samples are displayed in Fig. 2. These provide a qualitative measure of interface roughness and/or interdiffusion. By roughness we mean long-range (>10 Å) variations of the height of a given layer, which may be transmitted throughout the multilayer (correlated roughness). Interdiffusion suggests atomic scale variations of layer height, with possible interchange of Fe and V atoms across the interface. Specular

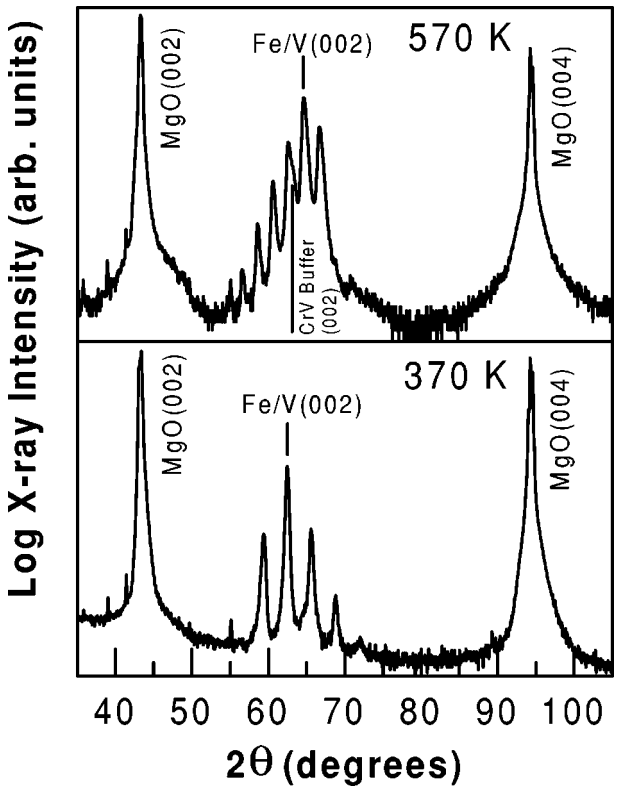

FIG. 1. High-angle specular x-ray diffraction scans from two Fe/V(001) superlattices. For either 570 K or 370 K growth, only (001) related features are observed, indicating the films have a single growth orientation. For both growth conditions, numerous superlattice satellites are observed around the main superlattice features.

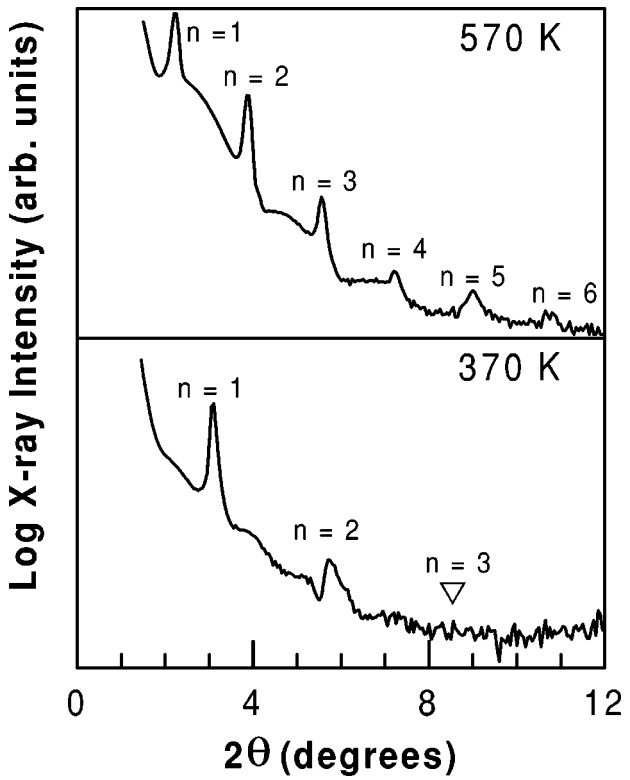

FIG. 2. Low-angle specular x-ray diffraction from the same films as in Fig. 1. The film deposited at 570 K shows 6 superlattice satellites out to $2\theta \approx 12°$, while the 370 K film shows no superlattice satellites beyond $\approx 6°$. This indicates more sharply modulated electron densities in the 570 K film.

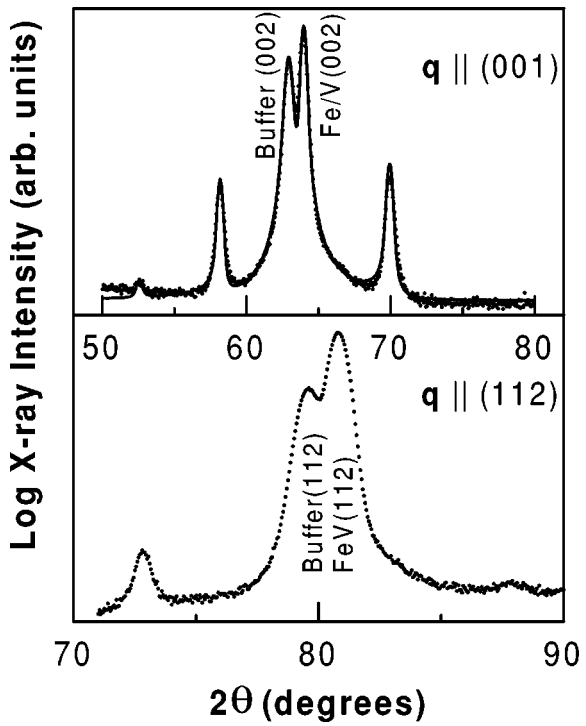

FIG. 3. Upper panel: High-resolution specular x-ray diffraction from an Fe/V(001) superlattice deposited at 570 K (symbols). The main superlattice (002) feature is surrounded by three satellites. The Cr-V buffer layer also presents a peak near 63°. The solid line represents a best fit to the data, as discussed in the text. Lower panel: Radial x-ray-diffraction scan through the superlattice (112) feature (scattering vector **q** inclined $\approx 35°$ to surface normal) of the same sample. From this scan we deduce that the superlattice film has very little tetragonal distortion, on average.

x-ray diffraction cannot distinguish between these two properties and measures a superposition of the two.

The spectrum of the sample grown at 570 K shows satellite features out to $\approx 12°$ in 2θ. This is typical for films deposited using the 570 K recipe. By comparison, the 370 K sample shows no features beyond $\approx 6°$ in 2θ, typical for the 370 K samples. From this we conclude that the 570 K samples have more sharply modulated electron densities along the growth direction.

A sample with 20 bilayer periods (consistent with samples used for magnetic characterization) was studied in detail by x-ray diffraction at West Virginia University, with structure: MgO(001)/25 Å Cr @ 870 K/300 Å Cr-V @ 570 K/11.5 Å Fe/$[6.2$ Å V/11.5 Å Fe$]_{20}$ @ 570 K/20 Å Si_3N_4. This sample was analyzed using a high-resolution four-circle diffractometer and Cu K_α radiation created by a rotating anode generator system.

In the upper panel of Fig. 3, a specular θ-2θ scan reveals five film-related peaks. The peak at 62.93°, corresponding to the (002) reflection, is associated with the Cr-V alloy buffer layer, indicating a lattice constant (LC) of 2.95 Å. This lies between the LC's of Cr (2.88 Å) and V (3.10 Å) in their bulk form, as expected for such an alloy. The rocking curve for this peak is $\approx 1°$ wide.

The main superlattice x-ray peak is located at 63.93° (LC = 2.91 Å). Its rocking curve is 0.82° wide, which indicates high quality epitaxial growth. Additionally, three superlattice satellites are seen (Fig. 3). The positions of the superlattice satellite peaks indicate a bilayer period of 17.7 Å.

To characterize the in-plane crystal structure, the superlattice reflection corresponding to the bcc (112) lattice constant was scanned using the four-circle goniometer. A θ–2θ scan of this reflection is shown in the lower panel of Fig. 3 (note that here the x-ray scattering wave vector **q** is canted by $\approx 35°$ with respect to the surface normal). The peak near $2\theta = 80.81°$ corresponds to the superlattice, while the smaller peak at $2\theta = 79.57°$ corresponds to the Cr buffer layer. Less intense peaks may correspond to superlattice satellites that are visible due to a limited long-range lateral coherence of the superlattice structure. Because only one (112) peak was observed corresponding to the superlattice, we can assume that both the V and Fe have an identical in-plane lattice parameter of 2.91 Å. This is identical to the lattice parameter along the surface normal. By comparison, the Cr-V alloy (peak position 79.57°) has an in-plane lattice spacing of 2.92 Å, and therefore has a slight tetragonal distortion of $\approx 1\%$.

A ϕ scan corresponding to the (112) superlattice reflection, shown in the upper panel of Fig. 4, reveals a four-fold in-plane symmetry. A similar ϕ scan of the buffer layer (112) reflection revealed the same four-fold in-plane symmetry, with the peaks located at the same values of ϕ. The lower panel also shows the MgO (113) peaks, which are offset by 45° with respect to the superlattice and buffer layer peaks. These scans confirm that this sample has a well-defined epitaxial relationship with the substrate, with

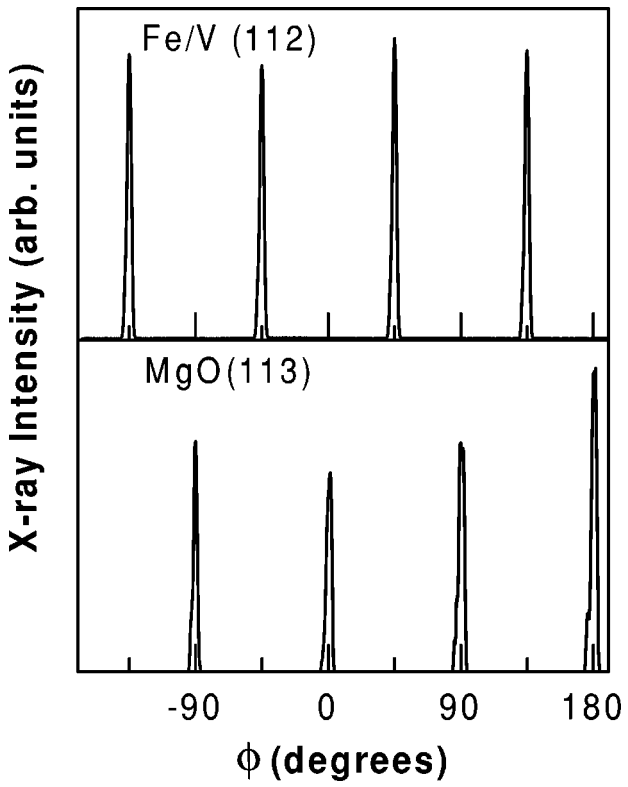

FIG. 4. Top: ϕ scan through the superlattice [112] peaks. Bottom: ϕ scan through the [113] features from the substrate. These scans demonstrate the epitaxial relationship between the film and substrate, namely, Fe/V(010) ‖ MgO(110).

Fe/V(010) ‖ Cr(010) ‖ MgO(110).

The x-ray scan with **q** along the [001] direction was quantitatively analyzed using the interdiffusion model developed by M. B. Stearns,[12] as implemented in the SUPREX computer program.[13] This model assumes that there is a linear change in the lattice constant and the atomic scattering factor at the interface of the two materials. The width of this interface corresponds to the sum of the roughness and interdiffusion. The in-plane lattice parameter determined from scans of the (112) peak (2.91 Å) was used to calculate the in-plane surface electronic density for the Fe and V. The number of monolayers of each material and their lattice constants were adjusted.

The best fit to the experimental data is shown as the solid curve in Fig. 3. The results indicate that the superlattice is composed of 11.5 Å of Fe and 6.2 Å of V, with perpendicular monolayer spacings of 1.42 Å for Fe and 1.52 Å for V. These values are equal to the bulk monolayer spacings of 1.43 Å for Fe and 1.52 Å for V within the fit uncertainty of 0.02 Å. Additionally, this is not far from what is calculated from the bulk Poisson ratios (0.293 and 0.365, respectively) for Fe and V. For an in-plane lattice spacing of 2.91 Å, one calculates Fe and V monolayer spacings of 1.43 and 1.56 Å, respectively. The difference between the expected V LC from Poisson's ratio and the actual measured value is not unusual in metallic superlattices, where deviations from Poisson's ratio have been observed in Nb/Cu, Nb/Al, W/Ni, and Mo/Ni, among other systems.[14]

The x-ray fit indicates significant interdiffusion even in the present superlattice, which was prepared under ''optimal'' conditions. The model structure has a first V layer that is actually composed of 40% Fe. The second V layer from the interface still has 10% Fe impurities. The two Fe layers closest to the interface have the same impurity levels. The Fe/V and V/Fe interfaces were not significantly different from one another. In a sense, the experimental multilayers have 4 ML of interdiffusion at the interfaces, although there is a strong compositional gradient in the interdiffused region.

Note that the diffusion profile determined here is very different from that modeled in the calculations simulating interdiffusion. The experimental profile is much broader, has a composition gradient, and has no chemical order. The calculations assumed a single layer of chemically ordered FeV alloy at the interface. These differences will be important below when we make comparisons between experiment and theory.

V. KERR MAGNETOMETRY

The bulk magnetic properties of all samples were characterized by magneto-optic Kerr effect (MOKE) magnetometry. All samples showed a four-fold in-plane magnetic anisotropy. The easy axes were aligned with the superlattice [100] and [010] directions. Representative MOKE loops from 570 K Fe/V superlattices are shown in Fig. 5. Easy axis magnetic loops, as a function of V layer thickness t_V, sometimes showed high saturation fields, indicating AF coupling between Fe layers.

The optimal (570 K) Fe/V superlattices showed a well-defined saturation field for all V thicknesses, which is plotted in Fig. 6, along with the zero-field remanence. We observe three peaks in saturation field as a function of t_V, at 22, 32, and 42 Å thickness. These peaks are strongly correlated with remanence minima. This combination of high saturation field and low remanence is associated with regions of AF coupling between Fe layers. The fact that such well-defined AF coupling peaks are observed out to $t_V \approx 50$ Å is another indicator of the high quality of these Fe/V superlattices.

Such AF coupling was previously observed in poly crystalline Fe/V multilayers,[15] but has not been observed previously in epitaxial (001) oriented Fe/V superlattices.[16,7] Specifically, previous measurements of epitaxial Fe/V showed no evidence for AF coupling in the range $t_V = 0-18$ Å.[16] In line with this, a striking feature in the present data is the absence of an expected AF coupling peak at $\approx$ 12 Å. It is surprising that this peak would be absent, since the oscillatory Ruderman-Kittel-Kasuya-Yosida (RKKY) coupling is expected to be strongest for thin V layers. Nevertheless, another type of coupling appears to suppress the AF coupling in this thickness range. This other effect must be more short ranged than the RKKY coupling, since AF coupling is easily observed for greater t_V. We hypothesize that this competing factor is direct exchange coupling between V atoms in the layer. This hypothesis is supported by both theoretical and experimental measurements of the V moments, presented in Sec. VI. As discussed in Sec. VII, it seems unlikely that direct coupling via pinholes is the origin of the absence of the AF peak at 12 Å.

We fit the peaks of the saturation field with the function

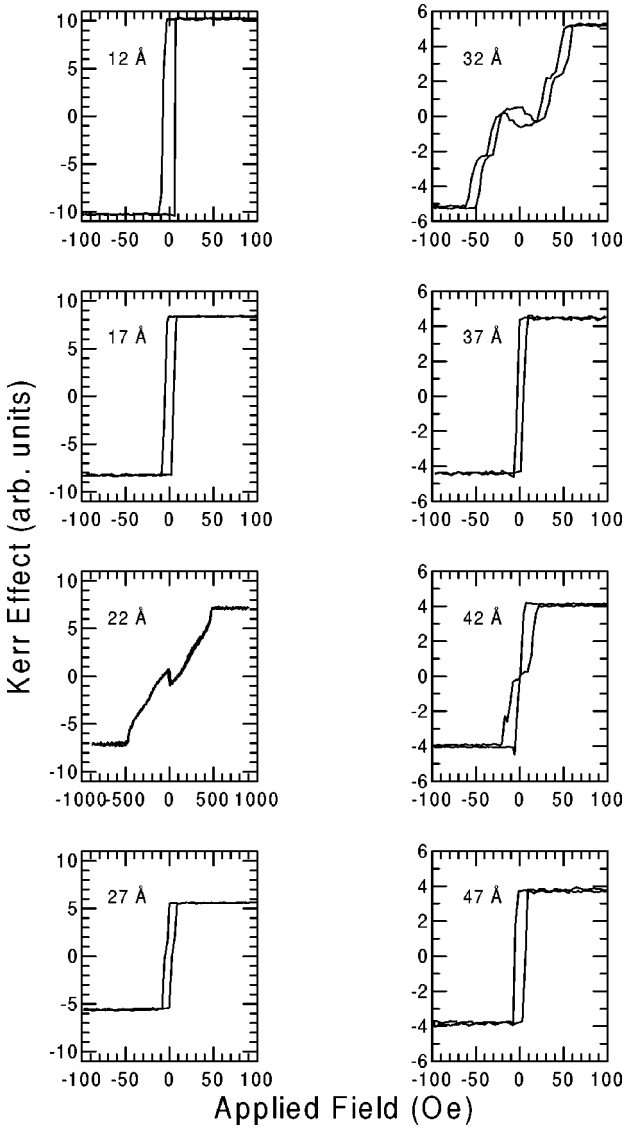

FIG. 5. Easy-axis magneto-optic Kerr effect loops from [Fe 10 Å/V t_V] superlattices. Three regions of antiferromagnetic coupling are observed at $t_V = 22$, 32, and 42 Å. Interestingly, these loops show negative remanence in the AF coupled regions. Note the change of vertical scale between left and right panels, and the change of horizontal scale for the $t_V = 22$ Å loop.

$$H_{\mathrm{sat}}^{\mathrm{peak}} = A\frac{\exp[-t_V/\lambda]}{t_V^2} + C \qquad (1)$$

(dashed line curve in Fig. 6). Here $A = 6.5\times10^6$ Oe, $\lambda = 7.9$ Å, and $C = 20$ Oe. The first term has the form of the envelope of an RKKY-type oscillatory coupling, damped by an exponential factor that represents the effect of lattice incoherency. The (small) offset field may be viewed as representing effects other than interlayer exchange coupling that determine the saturation field observed, such as coercivity. From this fit it would follow that in the absence of the ferromagnetic short-range direct exchange coupling the saturation field at the first AF coupling peak, which would then be observable, would be $\approx$ 10 kOe.

As an interesting aside, we point out that in the AF coupled regions many easy-axis loops (Fig. 5) displayed the

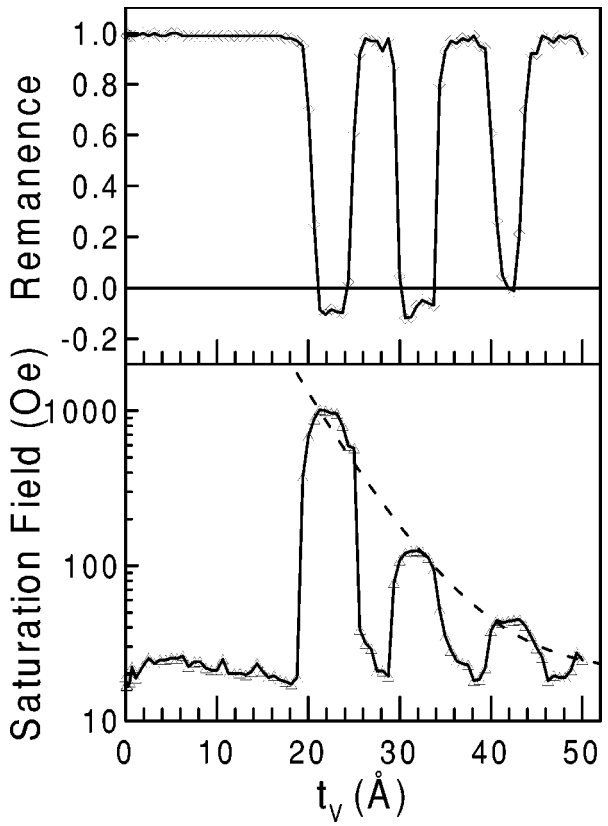

FIG. 6. Remanence and saturation field taken from loops as those in Fig. 5. Here the regions of AF coupling are well defined by high saturation fields and low remanence values (note negative remanence values in AF regions). The peaks in the saturation field are fit with an empirical function (see text).

so-called ''negative remanence'' effect.[17–20] The regions of negative remanence are clearly observed in Fig. 6. This is sometimes observed in magnetic multilayers with AF coupling. One explanation invokes magnetic moment variations *and* magnetic anisotropy variations from layer to layer to explain this effect.[20] More specifically, the layers carrying the larger moment must have the smaller magnetic anisotropy. Hence the AF coupling causes them to switch away from the applied field direction as the magnetic field is reduced to zero, leaving the low-moment layers aligned with the field.[20] The moment/anisotropy variations need not be large for negative remanence to occur, and we do not believe such variations impact the other results presented here.

Finally, note that in Fig. 5 the AF coupled loops corresponding to 22 and 32 Å thickness show a step roughly halfway between remanence and saturation. This is caused by the four-fold anisotropy within the multilayer film. As the film switches between AF and ferromagnetic alignment with increasing field, it pauses at the point where alternating layers have 90° alignment. At 90° alignment, all magnetic layers may have their moments aligned along an easy axis, representing a minimum in the anisotropy energy. In this state, half the layers are aligned with the field, and half are aligned $\approx$ 90° to the field, hence this point has a magnetization value equal to half the saturation value, as is observed.

VI. XMCD

X-ray magnetic circular dichroism (XMCD) measurements were performed at the Synchrotron Radiation Center,

at the University of Wisconsin-Madison. Approximately 85% circularly polarized x radiation allowed direct measurement of both Fe and V magnetic moments. This radiation was incident with an angle of 45° with respect to the surface normal, and the plane of incidence was parallel to the magnetic easy axis. An electromagnet switched the magnetization direction along this easy axis at each photon energy, with measurements taken in remanence. (As seen in Figs. 5 and 6, the remanent state of these films is still fully saturated for $t_V \lesssim 18$ Å.) The total electron yield of each sample was normalized to the yield from a Cu or Ni mesh, resulting in x-ray-absorption spectra. The difference in the x-ray-absorption spectrum for the two magnetization directions is the XMCD.

It is now well established that the magnitude of the XMCD is nearly proportional to the magnetic moment for a given element, independent of the magnitude of that moment. This was first elucidated for the spin moment (dominant in transition metals) in Ref. 21. This can be understood from the fact that the shape of the band structure of an element changes only slightly with a variation of the occupation number of spin-up and spin-down bands. In the present study, experimental proof of the latter point is found in the fact that the complicated *shape* of the V XMCD spectrum is exactly the same (to within experimental error) for all the samples discussed here, regardless of magnetic moment.

Thus, the relative size of the V (or Fe) magnetic moment is easily extracted for comparison between samples. With an additional measurement of a ''standard'' sample, where the magnetic moment is known, it becomes possible to extract absolute magnetic moments. To objectify the XMCD magnitude measurement, we compare the XMCD spectrum of each sample to that from the standard. The standard spectrum is scaled to achieve the best fit with that of the sample. This scaling factor then represents the magnitude of the moment in the sample, in terms of the moment in the standard. For a more complete explanation of this process, see Refs. 22 and 23.

The XMCD-determined magnetic moments contain at least two independent sources of error. One is a statistical error, which can be estimated from the quality of fit between the sample and standard spectra. This statistical error estimate is used to generate the error bars shown in the figures below. This error quantifies the reproducibility of the XMCD measurement itself. A second, larger, source of error comes from the assumed proportionality between the XMCD and magnetic moment. This ''systematic'' error has been discussed previously[24,22] and arises from (1) variations of the spin moment relative to the orbital magnetic moment, and (2) variations of the spin moment relative to the magnetic dipole correction term. In the worst case, such systematic errors may amount to 20% of the moment determination.[24,22]

A third source of error, important only for the V moments, comes from the standard sample. Since V is not normally magnetic, the measurement of a standard with a known magnetic moment is problematic. To provide the best calibration of V moment, we present data taken on Fe-V alloys over a range of compositions. By comparing these data with previous neutron-scattering measurements and with calculations, we obtain our best estimate of the proportionality constant between the V XMCD and its magnetic moment.

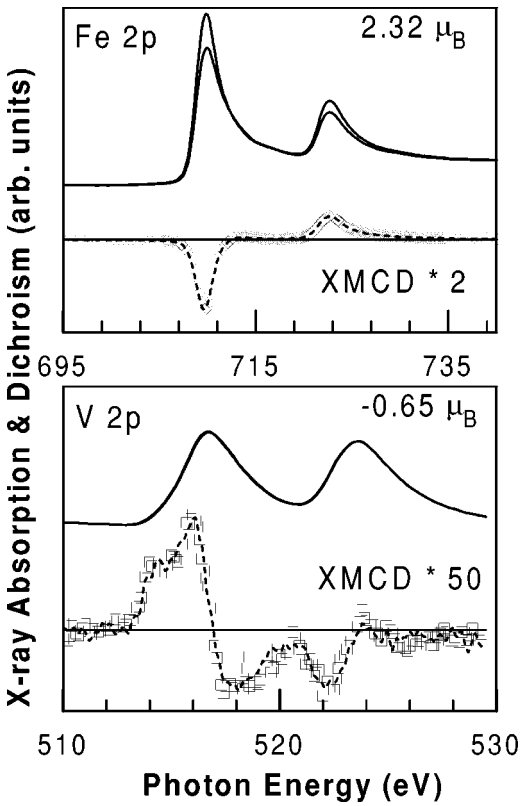

FIG. 7. X-ray absorption (solid lines) and dichroism spectra (symbols) from an Fe/V superlattice. The magnitude of the dichroism effect is a direct measure of the Fe and V magnetic moments. For each element, the dichroism data is overlaid with a scaled ''standard'' dichroism spectrum (dashed line) that is used to deduce the absolute Fe and V magnetic moments.

In Fig. 7 we present examples of XMCD spectra taken at the Fe and V absorption edges in an [Fe 10 Å/V 5 Å] superlattice film. By comparison with standard spectra (see below) we deduce average Fe and V moments of $2.32\mu_B$ and $-0.65\mu_B$, respectively. Each XMCD spectrum (symbols) is overlaid with a standard spectrum (solid curve) that has been scaled to match the data.

A. Fe-V alloy moments

To set the proportionality constant between V XMCD and V moment, we have pursued a study of Fe-V alloys, for which previous experimental[2] and theoretical[3] studies have been performed.

Figure 8 displays the XMCD-determined Fe and V magnetic moments in a series of Fe-V random alloys (symbols). Error bars are shown only for V and indicate the statistical reproducibility of the XMCD measurement (see above). The statistical error bars for the Fe moments were smaller than the symbols shown. The ordinate axis scale for the Fe data was set by comparison to a thick Fe(001) film, capped with a 20 Å Al layer. To make contact with previous results,[7] the standardization for V is initially chosen to be the same as in that paper.

Overlaying the XMCD data are the results of spin-polarized neutron-scattering measurements by Mirebeau and

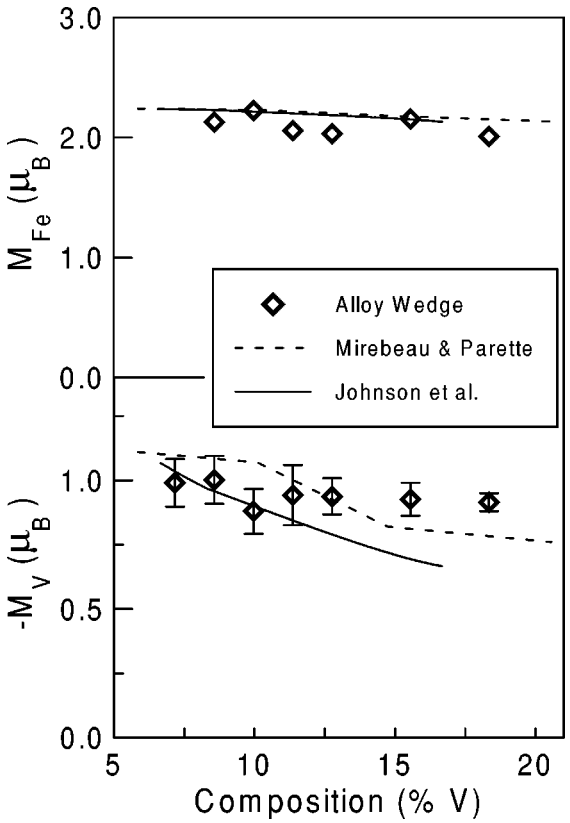

FIG. 8. Magnetic moments in Fe-V alloys as determined by XMCD. The Fe moments are hardly changed from bulk values. This graph sets the y-axis scale, i.e., the proportionality constant between the measured XMCD and magnetic moment for V. By comparison with previous experiments [Mirebeau and Parette Ref. 2] and theory [Johnson and co-workers Ref. 3] the XMCD scaling factor is adjusted to achieve agreement. Here we find that the best scaling factor is not significantly different from that used in a previous publication (Ref. 6).

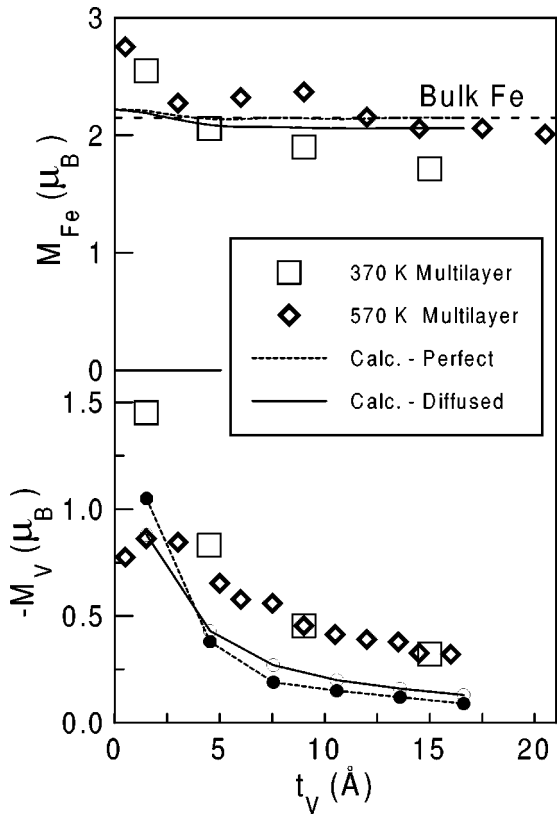

FIG. 9. Magnetic moments in Fe/V(001) superlattices as determined by XMCD. Again, the Fe magnetic moments are hardly changed from the bulk Fe value. The experimentally determined V moments are relatively large, and they decay monotonically with increasing t_V. The experiments are compared with calculations of perfect and diffused superlattices. Interdiffusion leads to higher V moments for most calculations. The experimental moments are still higher, partly due to greater interdiffusion and disorder in the experimental multilayers.

Parette (MP) (Ref. 2) (dashed line). (Note that the MP data presented here supersede data presented by the same group in Ref. 1). The data here are in good agreement with the MP data, without any change of scaling factor applied to the present results.

Additionally, the results of theoretical calculations of Johnson and co-workers, taken from Ref. 3, are overlaid as a solid line. The calculations show good agreement with the present data, though the agreement is slightly improved when the experimental XMCD results are scaled down by $\approx$ 15%.

These two comparisons suggest that our choice of proportionality constant relating the V XMCD and V moment is essentially correct, especially considering the other, systematic, errors mentioned above. Therefore, we choose to use exactly the same proportionality constant that was applied in Ref. 7. This proportionality constant is used in the next section for the determination of the V moments in Fe/V superlattices.

B. Superlattice moments

Figure 9 displays the Fe and V moments in the (001) oriented superlattices. When the V layers are $\leqslant$ 1 ML (1.5 Å), the Fe XMCD is substantially enhanced. For the thinnest interlayers, we have observed a similar Fe XMCD enhancement for Fe/Cr (Ref. 22) and Fe/Rh (Ref. 23), but not for Fe/Ru.[25]

Beyond 1 ML V, the Fe XMCD varies only a little from that of bulk Fe. Moreover, the Fe moments from the rougher 370 K films are very similar to the moments in the optimized 570 K films, in spite of the different Fe layer thicknesses for these samples. This is essentially in agreement with calculations of the Fe moments (both for perfect and diffused interfaces, see Fig. 9).

Moving now to the V moments, we find that the V atoms carry a relatively large magnetic moment, especially for small V thicknesses (Fig. 9). The growth recipe is an important factor for the V moments only when the V is thin. This is sensible, since the interface makes up a larger fraction of the V film for small t_V. The largest average V moment we have ever measured ($\approx 1.5\mu_B$) is observed in superlattice films with $t_V = 1.5$ Å deposited at 370 K. Similarly large moments are observed for analogous films deposited with (211) and (110) orientations.[7] Here the Fe/V interdiffused region is larger than the total V thickness. Yet these V moments are larger than in dilute V alloys ($\approx 1\mu_B$), and also

larger than in more perfect Fe/V superlattices. Somehow, the 370 K growth conditions have led to a maximization of the V moment.

Before turning to the calculational results, we emphasize that the experimental ones cannot be explained based on a simple model assuming alloyed interfaces. Using the x-ray-diffraction results for the interface composition, one could assign a V magnetic moment to each interface layer depending on its alloy composition. However, it was found that the average V moment in this model decays much too quickly to be of use. Furthermore, such a model could never predict the $1.5\mu_B$ moment mentioned above, since it is larger than the observed moments for any alloy composition.

The closest comparison of experiment and theory is between the 570 K superlattices and the diffused calculation. We observe that the experimental V moments are in fair agreement with the calculated values for thin V layers, where all of the V is alloyed, but that they are enhanced by more than 100% for the largest V thicknesses considered. Recall that the experimental diffusion profile is broader than that used for the calculation. Moreover, the interdiffusion in the experiment has a composition gradient and is chemically disordered, while the calculation assumed 1 ML of ordered alloy. This may partly explain the difference between the experimentally and theoretically determined V moments.

However, it is not expected that more interface roughness would lead to dramatically (factor of 2) higher V moments in the calculations. As the interdiffused region becomes thicker, it begins to resemble an Fe-V alloy that has lower Fe and V magnetic moments. Theoretically, we should consider other ways in which the structures assumed for calculations may be different from those in the experiments. Recall that we find that deformation of the V sublattice does not have a strong influence on the V moments calculated (Table I). Thus we have no explanation for the larger than expected differences between experimentally and theoretically determined V moments.

As a final comparison, we observe that the calculations of diffused superlattices typically show larger V moments than the calculations of perfect superlattices. For $t_V > 3$ ML, interdiffusion enhances the V moment by 30–40%. The only case where the perfect superlattice shows a higher V moment is for $t_V = 1$ ML. This can be understood by considering that the induced V moments are strongly correlated to the number of Fe nearest- and next-nearest-neighbor atoms, as discussed in Ref. 10 [see Fig. 9(b) in that paper]. At perfect interfaces, V atoms have 5 nearest- and next-nearest-neighbor Fe atoms, whereas V atoms in the mixed interface layers for $n > 3$ have 7 nearest- and next-nearest-neighbor Fe atoms. As the V moment of these atoms directly at the interfaces contribute strongly to the average V moment, the average moment is larger for systems with mixed interfaces than for systems with perfect interfaces. For the case $n = 1$, the V atoms in the perfect superlattice as well as those in the mixed interface layers have 10 nearest- and next-nearest-neighbor Fe atoms. The observed (relatively small) difference between the V moments for the two $n = 1$ structures can in this case apparently be understood only from a consideration beyond that on the total number of nearest neighbors.

To summarize, we find that the V magnetic moments typically increase with increasing interdiffusion. But only up to a point, as the V moment subsequently goes down for the random alloy (infinite diffusion). A point by point comparison of the superlattices discussed here with alloys having the same average composition readily verifies this statement. Hence, there is an intermediate diffusion level that maximizes the induced V magnetic moment in Fe/V superlattices.

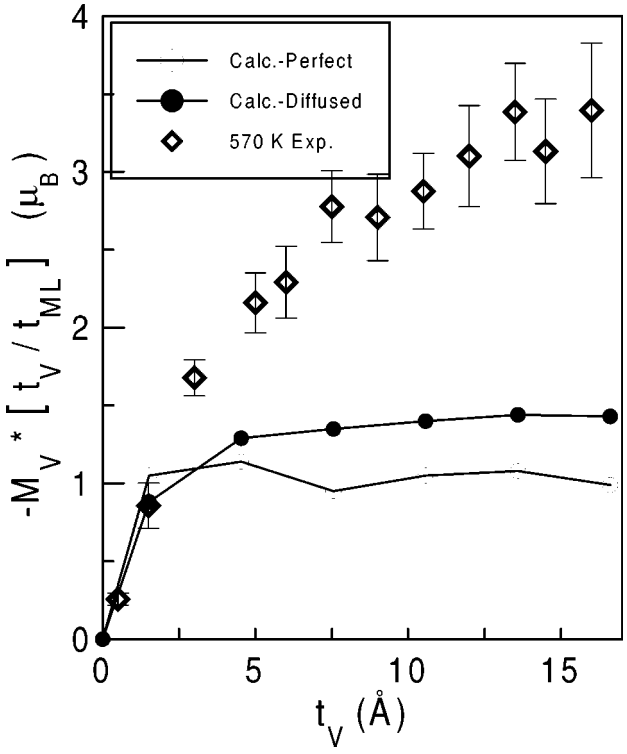

FIG. 10. The *layer integrated* V magnetic moment in the Fe/V superlattices. For calculations of perfect superlattices, this quantity saturates already at 4.5 Å (3 ML) V. This indicates that beyond this thickness, no additional V moment is added with increasing thickness. For calculations of diffused superlattices, this quantity does not saturate so quickly. The experimental measure of the quantity saturates even more slowly (only data from the 570 K multilayers are shown). This suggests that in the experiments, even the fourth V monolayer from the Fe interface possesses a significant moment, and that below 15 Å (10 ML), all V moments in the layer are ferromagnetically aligned.

VII. DISCUSSION

That the induced V moment can be so large is an interesting result, yet how is this moment distributed through the V layer? One way to obtain more information is to plot the total magnetic moment of the V layer (i.e., the average V moment multiplied by the equivalent number of V monolayers) versus t_V. This is done in Fig. 10.

Beginning with the calculation of perfect interfaces, we find that the total V moment saturates at about 4.5 Å (3 ML). Indeed, Table I shows small but oscillatory V moments in the interior of the V layer (i.e., transient antiferromagnetism).

For diffused interfaces, the calculations show a gradually increasing V moment with increasing t_V (Fig. 10), out to at least 10.5 Å (7 ML). As compared with calculations having perfect interfaces the individual layer moments extend to greater distances from the Fe/V interface, and are generally

larger in magnitude (Table II). Here the V is clearly in a transient ferromagnetic state.

This effect is even more apparent in the experiments (Fig. 10), which have greater interdiffusion. It is clear that the total V magnetic moment is not saturated even at $t_V = 12$ Å (8 ML). Recall that at 12 Å thickness, we believe there are about 4 ML of pure V in the layer interior. Although we do not know the V moment profile, Fig. 10 suggests that at 12 Å, the innermost V monolayers still possess a non-negligible magnetic moment, and that this moment is aligned ferromagnetically with all the other V monolayers. This magnetic moment arises from direct exchange coupling between adjacent V atoms throughout the layer. The present results are distinct from results of thin V overlayers on Fe(001), which displayed oscillating V moments with increasing t_V.[4,5] Note that here the V layers are bounded on both sides by Fe, and this may explain the difference for V in the two cases.

We now have an explanation for the suppression of the first AF coupling peak between Fe layers at 12 Å V thickness (Sec. V). The direct exchange coupling between adjacent V monolayers competes with the indirect RKKY coupling between Fe layers. Direct coupling favors the ferromagnetically aligned state (observed), while the RKKY coupling favors AF alignment for this V thickness. From the analysis given in Sec. V it follows that at $t_V = 12$ Å the ferromagnetic coupling field (direct exchange interaction) is larger than about 10 kOe. Because the direct coupling is expected to fall more quickly with increasing thickness as compared with the RKKY coupling, the RKKY coupling dominates at the second, third, and fourth coupling peaks, so that these are observed.

We liken the behavior of the present V layers to the behavior of Pd layers in Fe/Pd superlattices. Pd is well known to be nearly ferromagnetic, and recent XMCD measurements indicate significant Pd moments extending up to 4 ML from the Fe interface.[26] In that system, the oscillating RKKY coupling is dominated by a ferromagnetic bias, which suppresses the first two AF coupling peaks (at about 6 and 10 ML), although a remnant of these peaks is visible as oscillations of the ferromagnetic coupling strength.[27] The ferromagnetic bias is certainly related to the long-ranged nature of the induced Pd moments. In the particular Fe/V superlattices under study here, interdiffusion supports a transient ferromagnetic state, and we argue that the long-ranged nature of the induced V moments is related to the suppression of the first AF coupling peak in the present study.

It is important to consider the possibility of Fe-containing pinholes within the V layers, which could cause direct ferromagnetic bridging between the Fe layers. If present, such bridging could suppress the first AF coupling peak. However, the x-ray-diffraction results indicate essentially zero Fe content in the third and fourth V monolayers away from the Fe/V interface. We therefore believe that pinholes do not play a significant role in determining the magnetic properties of the present films.

Still, interdiffusion between the Fe and V creates some ambiguity regarding the thickness of the ferromagnetic and nonmagnetic layers. This ''magnetic roughness'' causes a kind of frustration, which works to weaken the RKKY spin-density wave. At the same time, we have shown by calculations that interdiffusion destroys a tendency toward antiferromagnetism in the V layer. The experiments, which have still greater interdiffusion, exhibit transient ferromagnetism, suggesting strong ferromagnetic V-V direct exchange coupling. The coexistence of a weakened RKKY coupling and strengthened V-V direct exchange coupling leads to the suppression of the first AF coupling peak. Thus interdiffusion plays a key role in determining the magnetic properties of these superlattices.

VIII. CONCLUSION

We have performed experimental and theoretical studies of Fe/V(001) superlattices and alloys. Our main results are summarized as follows: (1) Finite interface interdiffusion favors an increased average V magnetic moment, as compared with either no interdiffusion (perfect superlattices) or infinite interdiffusion (alloys). (2) The measured V moments are characterized by a transient ferromagnetic state, with strong V-V direct exchange coupling. (3) This direct exchange coupling suppresses the first AF coupling peak between Fe layers at $t_V \approx 12$ Å. However, because the direct exchange coupling decays more quickly than the indirect RKKY coupling between Fe layers, three other AF coupling features are observed for greater t_V.

ACKNOWLEDGMENTS

The authors gratefully acknowledge support of the National Science Foundation CAREER Contract No. DMR-9623246. The Synchrotron Radiation Center is supported by the NSF under Contract No. DMR-9212658. One of the authors (M.M.S.) was partly supported by the Condensed Matter and Surface Science Program of Ohio University.

[1] K. Adachi, in *3d, 4d, and 5d Elements, Alloys, and Compounds*, Vol. 19a of *Landolt-Börnstein, New Series, Group 3*, edited by H. P. J. Wijn, (Springer-Verlag, Berlin, 1986), pp. 330–331.

[2] I. Mirebeau, G. Parette, and J. W. Cable, J. Phys. F **17**, 191 (1987).

[3] D. D. Johnson, F. J. Pinski, and J. B. Staunton, J. Appl. Phys. **61**, 3715 (1987).

[4] T. G. Walker and H. Hopster, Phys. Rev. B **49**, 7687 (1994).

[5] P. Fuchs, K. Totland, and M. Landolt, Phys. Rev. B **53**, 9123 (1996).

[6] G. R. Harp, S. S. P. Parkin, W. L. O'Brien, and B. P. Tonner, Phys. Rev. B **51**, 3293 (1995).

[7] M. A. Tomaz, W. J. Antel Jr., W. L. O'Brien, and G. R. Harp, J. Phys.: Condens. Matter **9**, L179 (1997).

[8] N. Hamada, K. Terakura, and A. Yanase, J. Phys. F **14**, 2371 (1984).

[9] A. Vega, A. Rubio, L. C. Balbas, J. Dorantes-Davila, S. Bouarab, C. Demangeat, A. Mokrani, and H. Dreyessé, J. Appl. Phys. **69**, 4544 (1991).

[10] R. Coehoorn, J. Magn. Magn. Mater. **151**, 341 (1995).

[11] L.-C. Duda, P. Isberg, S. Mirbt, J.-H. Guo, B. Hjörvarsson, J. Nordgren, and P. Granberg, Phys. Rev. B **54**, 10 393 (1996).
[12] M. B. Stearns, Phys. Rev. B **38**, 8109 (1988).
[13] E. E. Fullerton, I. K. Schuller, H. Vanderstraeten, and Y. Bruynseraede, Phys. Rev. B **45**, 9292 (1992).
[14] A. Fartash, M. Grimsditch, E. E. Fullerton, and I. K. Schuller, Phys. Rev. B **47**, 12 813 (1993); A. Fartash, I. K. Schuller, and M. Grimsditch, in *Evolution of Surface & Thin Film Microstructures Symposium*, edited by H. A. Atwater, E. Chason, M. H. Grabow, and M. G. Lagally, MRS Symposia Proceedings No. 280 (Materials Research Society, Pittsburgh, 1993).
[15] S. S. P. Parkin, Phys. Rev. Lett. **67**, 3598 (1991).
[16] P. Granberg, P. Nordblad, P. Isberg, B. Hjörvarsson, and R. Wäppling, Phys. Rev. B **54**, 1199 (1996).
[17] C. Gao and M. J. O'Shea, J. Magn. Magn. Mater. **127**, 181 (1993).
[18] M. J. O'Shea and A.-L. Al-Sharif, J. Appl. Phys. **75**, 6673 (1994).
[19] X. Yan and Y. Xu, J. Appl. Phys. **79**, 6013 (1996).
[20] H. Theuss, T. Becker, D. Weller, and H. Kronmuller, J. Appl. Phys. **81**, 3914 (1997).
[21] Paolo Carra, B. T. Thole, Massimo Altarelli, and Xindong Wang, Phys. Rev. Lett. **70**, 694 (1993).
[22] M. A. Tomaz, W. J. Antel Jr., W. L. O'Brien, and G. R. Harp, Phys. Rev. B **55**, 3716 (1997).
[23] M. A. Tomaz, D. C. Ingram, G. R. Harp, D. Lederman, E. Mayo, and W. L. O'Brien, Phys. Rev. B **56**, 5474 (1997).
[24] D. Weller, J. Stöhr, R. Nakajima, A. Carl, M. G. Samant, C. Chappert, R. Megy, P. Beauvillian, F. Viellet, and G. Held, Phys. Rev. Lett. **75**, 3752 (1995).
[25] Tao Lin, M. A. Tomaz, M. M. Schwickert, and G. R. Harp, Phys. Rev. B (to be published).
[26] Jan Vogel, A. Fontaine, V. Cros, F. Petroff, J.-P. Kappler, G. Krill, A. Rogalev, and J. Goulon, Phys. Rev. B **55**, 3663 (1997).
[27] Z. Celinski, B. Heinrich, and J. F. Cochran, J. Appl. Phys. **70**, 5870 (1991).